1   Target Journal: **Royal Society Interface**

2   Title: **Which lower-limb joints compensate for destabilising energy during walking in humans?**

3   Authors: *Pawel R. Golyski[a,b], Gregory S. Sawicki[a,b,c,d]

4

5   Affiliations:

6   [a] Parker H. Petit Institute for Bioengineering and Biosciences, Georgia Institute of Technology, Atlanta,

7   GA, USA

8   [b] George W. Woodruff School of Mechanical Engineering, Georgia Institute of Technology, Atlanta, GA,

9   USA

10   [c] Institute for Robotics and Intelligent Machines, Georgia Institute of Technology, Atlanta, GA, USA

11   [d] School of Biological Sciences, Georgia Institute of Technology, Atlanta, GA, USA

12   *Corresponding Author.

13   E-mail: pgolyski3@gatech.edu

14

15   ORCID

16   Pawel R. Golyski: 0000-0001-9844-2859

17   Gregory S. Sawicki: 0000-0002-5588-6297

18

19   **Abstract Word Count: 199/200**

20   **Word Limit (Research): 5838/8000**

21   **Number of References: 57**

22

23

24   **Abstract:** Maintaining stability during perturbed locomotion requires coordinated responses across

25   multiple levels of organization (*e.g.,* legs, joints, muscle-tendon units). However, current approaches to

26   investigating such responses lack a "common currency" that is both shared across scales and can be

27   directly related to perturbation demands. We used mechanical energetics to investigate the demands

28   imposed on a leg by a transient increase in unilateral treadmill belt speed targeted to either early or late

29   stance. We collected full body kinematics and kinetics from 7 healthy participants during 222 total

30   perturbations. From across-subject means, we found early stance perturbations elicited no change in

31   net work exchanged between the perturbed leg and the treadmill but net positive work at the overall

32   leg level, and late stance perturbations elicited positive work at the leg/treadmill interface but no

33   change in net work at the overall leg level. Across all perturbations, changes in ankle and knee work

34   from steady state best reflected changes in overall leg work on the perturbed and contralateral sides,

35   respectively. Broadening this paradigm to include joint level (vs. leg level) perturbations and including

36   muscle-tendon unit mechanical energetics may reveal neuromechanical responses used in destabilizing

37   environments which could inform design of balance-assisting devices and interventions.

38

41

42

1. Introduction

Falls remain a major public health problem. In the United States alone, 1 in 4 adults over 65 years old fall at least once a year, which result in over 25,000 deaths annually and $31 billion in annual direct healthcare costs [1–3]. In the workplace, falls caused 16% of fatal work-related injuries in 2019, with 68% of fall-related injuries occurring in individuals between 35 and 64 years old [4,5]. In both younger and older adults, falls occur more often during walking than any other locomotor task, with external disturbances such as slips and trips being the predominant perceived cause of falls [6,7]. Although responses to external perturbations have been extensively studied at the scales of the overall leg (*i.e.*, foot placement), joints, and muscles (*e.g.*, [8–17]), how stabilizing responses are related and coordinated *across scales* is not well understood. Two obstacles to such analyses are: 1) variables used to characterise responses are generally not measured using a "common currency" that can be easily related across different scales, and 2) the explicit, quantifiable demand imposed by the perturbation is unknown. In this work we aimed to overcome these obstacles by using a split-belt treadmill to deliver destabilizing perturbations using transient changes in belt speed that imposed quantifiable energetic demands on the legs that could be related to changes in work at the joints. We anticipate this analysis will serve as an initial step in multi-scale analysis of stability through mechanical energetics.

The mechanical power of each leg during walking, with respect to a fixed global reference frame and assuming massless legs, can be estimated using the individual limbs method [18], which quantifies the mechanical energy flowing between the ground and the centre of mass (COM). During overground walking, the mechanical power of each leg is the dot product of its corresponding ground reaction force (GRF) and COM velocity. No power flows between each leg and the ground because the velocity of the ground is 0, thus $F_{Leg} \cdot v_{ground} = 0$, where F_{Leg} is equal and opposite to the ground reaction force. However, for treadmill walking, this is no longer the case; with respect to a fixed global reference frame,

66   each belt is moving, so the power flowing from each leg to its corresponding belt is $F_{Leg} \cdot v_{belt}$. Thus, in

67   the case of treadmill walking, the mechanical power of each leg is the sum of the power flowing from

68   the leg to the treadmill belt and the leg to the COM [19].

69   During level ground treadmill walking with both belts of a split-belt treadmill moving at the

70   same speed, the net work of each leg on the COM is zero on average over a stride. Further, with both

71   belts moving at the same speed, since the average anteroposterior force must be zero over a stride

72   (otherwise the COM would accelerate relative to the treadmill), each leg performs zero net mechanical

73   work on its corresponding belt. Therefore, in this condition the net work performed by each leg must be

74   zero on average [20]. However, in either non-steady conditions or when belts of a split-belt treadmill are

75   moving at different speeds, the previous assumptions no longer hold, and a treadmill can elicit an

76   energetic demand on the leg over a stride. In this work, we leveraged this concept and designed

77   perturbations intended to elicit a change in net work over a stride by a leg (*i.e.* generation or

78   dissipation). Specifically, since leg force is directed anteriorly in early stance and posteriorly in late

79   stance, by increasing the posterior velocity of a belt our first hypothesis was net negative work would be

80   elicited over a stride at the leg/treadmill interface with an early stance perturbation, while net positive

81   work would be elicited over a stride with a late stance perturbation (figure 1). Our second hypothesis

82   was that such changes in net work at the leg/treadmill interface relative to an unperturbed stride would

83   be reflected at the level of overall leg work, since the treadmill environment limits large fluctuations in

84   COM velocity and thus mechanical power exchanged between each leg and the COM ($F_{GRF} \cdot v_{COM}$).

85   While no previous work has investigated the mechanical energetics of transient unilateral

86   treadmill speed perturbations during walking, there are numerous experimental contexts that elicit an

87   energetic demand on the legs during locomotion by changing the required amount of work the legs

88   perform on the COM. Examples include increasing or decreasing the slope of the ground relative to level

89   [21–25], accelerating or decelerating [26,27], and falling into a hole [28,29]. In general, relative to level

90   ground, walking on an incline results in a shift to more positive work and power at the hip joint [21–24],

91   while walking on a decline results in more negative work and power at the knee joint [22–24]. However,

92   in the case of speed changes and ground height perturbations, changes in ankle work and power best

93   reflect the overall demand on the leg [26–30]. Since our perturbations were more similar to speed

94   changes than slope changes, our third hypothesis was that changes in net leg work over a stride

95   resulting from the perturbation would primarily be reflected by changes in net work at the ankle joint.

96   **2. Methods**

97   **2.1 Experimental protocol**

98   Seven young, healthy individuals (5 males, 2 females, mean [SD]: 25 [2] years, 178.5 [12.1] cm

99   stature, 72.7 [13.3] kg) walked on an instrumented split-belt treadmill (CAREN; Motek, Netherlands).

100   Following an unperturbed 5-minute acclimation period at 1.25 m/s [31], transient unilateral belt

101   accelerations were delivered during walking. Each perturbation was targeted to either early or late

102   stance and either the left or right leg. Each timing/leg pairing was repeated 10 times (*i.e.*, 2 legs x 2

103   timings x 10 repetitions = 40 perturbations per participant). The order of perturbations was randomized,

104   with 30-40 steps between perturbations to ensure the perturbation was unexpected and the participant

105   had returned to steady state walking [32]. The perturbation algorithm is fully described elsewhere [33],

106   and used real-time kinematic data to estimate gait phase during walking. Perturbations consisted of a

107   brief (mean duration: 340 ms, 32.9% perturbed gait cycle) increase in belt speed from 1.25 m/s to 2.5

108   m/s (figure 1B). All participants provided informed consent as approved by the local Institutional Review

109   Board.

110   [Figure 1 about here]

111   **2.2 Kinematics and kinetics**

112   67 reflective markers (modified Human Body Model 2; [34]) were placed on the bony landmarks

113   and major body segments (head, hands, forearms, upper arms, torso, pelvis, thighs, shanks, and feet) of

114   each participant. A 10-camera motion capture system (Vicon; Oxford, UK) collected 3D marker

115   trajectories at 200 Hz. For each participant, a static trial was used to scale an individualized version of

116   the generic full body musculoskeletal model developed by Rajagopal and colleagues (37 degrees of

117   freedom, 22 rigid bodies; [35]). The metatarsophalangeal and subtalar joints of the models were locked

118   in all analyses, thereby assuming the foot was a rigid body. These subject specific models, in conjunction

119   with measured marker positions, were used to calculate joint angles for each trial using the inverse

120   kinematics tool in OpenSim v. 4.0 [36]. Joint moments were calculated with the inverse dynamics tool in

121   OpenSim using both the joint angles and bilateral ground reaction forces (2000 Hz sampling) applied to

122   the calcanei of the scaled models. Joint kinematics and kinetics were lowpass filtered using 4th order

123   zero-phase Butterworth filters at 6 and 15 Hz, respectively. Strides were segmented using a 30 N

124   threshold from vertical ground reaction forces. Trials where participants crossed over the belts, as

125   determined by manual inspection, were removed from analysis, leaving 222 successful trials.

126   **2.3 Mechanical energetics**

127   Joint powers were calculated as the product of joint moments and joint angular velocities. To

128   estimate leg power from summed joint power, joint powers about each available degree of freedom

129   were summed (ankle plantar/dorsiflexion, knee flexion/extension, hip flexion/extension, hip

130   ab/adduction, and hip external/internal rotation). To estimate leg power most accurately from joint

131   power, 6 degree of freedom joint powers and a deformable segment model for the foot are preferred

132   [37–40], but such calculations are not compatible with model-based OpenSim analysis that constrains

133   joints to behave within physiological bounds. Thus, an additional "ground-truth" estimate of leg power

134   was calculated using a modified individual limbs method [18,19,37]. This corrected leg power was the

135   sum of 1) the power flowing from each leg to the treadmill, 2) the power flowing from each leg to the

136   COM, and 3) the peripheral power of the leg segments (thigh, shank, and foot) relative to the COM. The

137   power from the leg to the treadmill was calculated as the dot product of the force from each leg on the

138   ground (equal and opposite to ground reaction force) with the velocity of the respective treadmill belt

139   (logged at approximately 70 Hz). The power from each leg to the COM was calculated as the dot product

140   of each ground reaction force and the velocity of the whole-body COM as calculated by the Body

141   Kinematics tool in OpenSim. This kinematic COM estimate was selected instead of estimates based on

142   GRF [18–20] because GRF-based estimates of COM velocity solve for integration constants assuming

143   steady-state behaviour over multiple strides, but such integration constants may not be valid during

144   perturbed strides. Peripheral power of the leg segments was calculated by summing the time derivative

145   of the rotational and translational components of kinetic energy [37,41,42]. Mechanical work at the

146   levels of the joints and legs was calculated using trapezoidal integration of joint powers.

147   **2.4 Statistical analysis**

148   All statistical analyses were performed in Matlab R2019b (Mathworks, Natick, MA, USA). To

149   characterize the influence of the perturbation, sagittal plane extrema in kinematic and kinetics, in

150   addition to mechanical work estimates, were evaluated using a linear mixed model with fixed effects of

151   perturbation timing (2 levels: early and late) and ipsilateral stride in relation to the perturbation [4

152   levels: S-1 (the preceding unperturbed, steady state stride), S0 (perturbed stride), S+1 (first recovery

153   stride), S+2 (second recovery stride)], in addition to a random effect of participant. Bonferroni-corrected

154   pairwise t-tests were run for *post-hoc* analyses. Linear regressions were used to relate changes in

155   corrected leg work with changes in ankle, knee, and hip work. For these regressions, changes in leg and

156   joint work were calculated relative to steady state strides (*i.e.*, the work of stride S+N – work of stride S-

157   1). Significance was concluded for p-values ≤ 0.05.

158   **3. Results**

3.1 Peak joint angles

Significant timing x stride interactions were observed in ipsilateral ankle, knee, and hip angles, in addition to contralateral ankle and knee angles (electronic supplementary material, table S1). Differences in kinematics following the perturbation relative to steady state (S-1) were predominantly limited to the perturbed stride (S0) and first recovery stride (S+1; figure 2).

On the perturbed stride (S0) and ipsilateral leg, both early and late stance perturbations resulted in increased plantarflexion (both timings: $p < 0.001$), knee flexion (early: $p = 0.030$, late: $p < 0.001$), and hip flexion (both timings: $p < 0.001$), with late stance perturbations causing larger deviations than early stance perturbations ($p < 0.001$ for all). During the perturbed stride (S0) on the contralateral leg there were similar increases in hip flexion for both timings (both timings: $p < 0.001$). However, early stance perturbations resulted in increased knee flexion at initial contact compared to late stance perturbations, evidenced by a decreased range of motion ($p < 0.001$), while late stance perturbations resulted in increased dorsiflexion compared to early stance perturbations ($p < 0.001$).

On the first recovery stride (S+1), increased ipsilateral hip flexion relative to steady state persisted for both timings (early: $p = 0.032$, late: $p < 0.001$), with deviations being larger for late vs. early stance perturbations ($p < 0.001$). Late stance perturbations also resulted in decreased hip extension ($p = 0.003$). On the contralateral leg, both perturbation timings resulted in decreased plantarflexion (early: $p = 0.003$, late: $p < 0.001$) and hip extension (both timings: $p < 0.001$), with larger deviations in plantarflexion following late compared to early stance perturbations ($p < 0.001$). Late stance perturbations also resulted in in increased dorsiflexion, decreased knee flexion, and increased hip flexion relative to steady state ($p < 0.001$ for all).

[Figure 2 about here]

3.2 Peak joint moments

182   Significant timing x stride interactions were observed in ipsilateral ankle, knee, and hip

183   moments, in addition to contralateral knee extension moments (electronic supplementary material,

184   table S1). Differences in joint moments following the perturbation relative to steady state (S-1) were

185   predominantly limited to the perturbed stride (S0; figure 3).

186   On the perturbed stride (S0) and ipsilateral leg, both early and late stance perturbations

187   resulted in increased knee flexion moments (early: $p = 0.013$, late: $p < 0.001$) and hip flexion moments

188   (both timings: $p < 0.001$), with late stance perturbations resulting in larger flexion moments than early

189   stance perturbations (both joints: $p < 0.001$). Late stance perturbations also resulted in increased ankle

190   plantarflexion moments ($p = 0.002$) and knee extension moments ($p < 0.001$). On the contralateral leg,

191   both early and late stance perturbations resulted in increased knee extension (both timings: $p < 0.001$),

192   knee flexion (early: $p = 0.005$, late: $p < 0.001$), and hip extension moments (both timings: $p < 0.001$),

193   with late vs. early stance perturbations eliciting larger deviations in knee extension moments ($p < 0.001$)

194   and knee flexion moments ($p = 0.002$) from steady state (S-1). Late stance perturbations were also

195   associated with decreased contralateral plantarflexion moments relative to steady state (S-1; $p = 0.019$).

196   [Figure 3 about here]

197   **3.3 Peak joint powers**

198   Significant timing x stride interactions were observed in peak mechanical power generation and

199   dissipation at all joints, apart from dissipation at the hip joint (electronic supplementary material, table

200   S1). Similar to joint moments, differences in joint powers following the perturbation relative to steady

201   state (S-1) were predominantly limited to the perturbed stride (S0; figure 4), with the exception of

202   altered power generation at the contralateral ankle in the first recovery stride (S+1).

203   On the perturbed stride (S0) and ipsilateral leg, both early and late stance perturbations

204   resulted in increased dissipation at the knee (both timings: $p < 0.001$) and both increased generation

205   and dissipation at the hip (p < 0.001 for all), with late vs. early stance perturbations being associated

206   with increased dissipation at the knee and increased generation at the hip (both joints: p < 0.001). Late

207   stance perturbations additionally resulted in both increased generation and dissipation at the ankle joint

208   (both signs: p < 0.001). The effects of both timings on the ipsilateral hip and knee were similar to the

209   effects on the contralateral joints: both early and late stance perturbations resulted in increased

210   dissipation at the knee (early: p = 0.002, late: p < 0.001), increased dissipation at the hip (both timings: p

211   < 0.001), and increased generation at the hip (early: p < 0.001, late: p = 0.015), with there being more

212   dissipation at the hip in late vs. early stance perturbations (p < 0.001). Further, early stance

213   perturbations resulted in increased dissipation at the contralateral ankle, while late stance perturbations

214   elicited increased generation at the contralateral knee (both joints: p < 0.001).

215   On the first recovery stride (S+1), the primary differences from steady state (S-1) were

216   decreased generation at the contralateral ankle (both timings: p < 0.001), with less generation for late

217   vs. early stance timings (p = 0.002), in addition to decreased generation at the ipsilateral knee for late

218   stance perturbations (p = 0.011).

219   **3.4 Leg mechanical energetics**

220   On the perturbed stride (S0) and ipsilateral leg, corrected leg powers better matched summed

221   joint powers for early vs. late stance perturbations (figure 5A, R^2 = 0.82 for early, R^2 = 0.54 for late).

222   Relative to steady state walking (S-1), early stance perturbations elicited more corrected leg work from

223   the perturbed leg on the perturbed stride (p = 0.001), while late stance perturbations did not elicit a

224   significant change in corrected leg work (p = 1.000; figure 5C). For early stance perturbations, this overall

225   increase in corrected leg work was mediated by an increase in work performed by the ipsilateral leg on

226   the COM (p < 0.001), while work performed by the leg on the treadmill was unchanged (p = 1.000). For

227   late stance perturbations, the unchanged overall work performed by the ipsilateral leg was due to

228   increased negative work performed by the leg on the COM ($p < 0.001$) being cancelled by more positive

229   work being performed by the leg on treadmill ($p = 0.005$). There was no change in peripheral leg work

230   for either perturbation timing ($p > 0.405$).

231   Relating individual joint work with corrected leg work suggests that on the perturbed stride,

232   changes in ipsilateral ankle ($R^2 = 0.56$, figure 6i) and contralateral knee work ($R^2 = 0.67$, figure 6ii) best

233   reflect changes in overall leg work as a result of the perturbation. On the first recovery stride, changes in

234   ipsilateral ankle ($R^2 = 0.60$, figure 6iii) and hip work ($R^2 = 0.39$, figure 6iv) best reflected changes in

235   corrected leg work.

236   **4. Discussion**

237   The overall objective of this work was to relate overall leg and joint level responses to

238   destabilizing perturbations during walking using mechanical energetics. We used a split-belt treadmill to

239   elicit transient mechanical energetic demands on the legs during walking and investigated which joints

240   best reflected those demands. Our first hypothesis was that unilateral belt accelerations delivered in

241   early or late stance would elicit net negative or positive work, respectively, from the perturbed leg at

242   the leg/treadmill interface over a stride. Our data supported this hypothesis for late stance

243   perturbations, but not for early stance perturbations. In the case of early stance perturbations, while

244   more negative power was elicited from the leg at the leg/treadmill interface in early stance, the

245   posterior movement of the leg caused by the perturbation led to a more posteriorly directed leg force

246   ([10] ,electronic supplementary material, figure S1). This posterior leg force resulted in more positive

247   power flowing from the leg to the treadmill in late stance, and no change in net work over a stride by

248   the perturbed leg on the treadmill belt. Thus, future work seeking to specifically elicit net negative work

249   at the leg/treadmill interface over a stride should consider decelerating the targeted treadmill belt

250   during late stance, thereby avoiding unexpected compensations to the perturbation.

251   Our second hypothesis was that changes in net work at the leg/treadmill interface over the

252   perturbed stride would be reflected by changes in overall leg work. Our data did not support this

253   hypothesis for either early or late stance perturbations. For early stance perturbations, which we initially

254   hypothesized would elicit net negative work from the perturbed leg, we found net *positive* work was

255   generated by the leg. This occurred due to the combined effect of the net zero work performed by the

256   leg on the treadmill coupled with less negative COM work in late stance. We attribute this decrease in

257   negative work to a combination of 1) the perturbed leg accelerating the COM forward, as evidenced by

258   an increased anteroposterior component of leg power, and 2) offloading of the perturbed leg around

259   toe-off resulting in decreased negative COM power (electronic supplementary material, figure S2). For

260   late stance perturbations, which we initially hypothesized would elicit net positive work from the

261   perturbed leg, we found no net change in work performed by the leg. In this case, the increased positive

262   work performed by the leg on the treadmill was offset by the increased negative work of the leg on the

263   COM in late stance. Increased negative COM power occurred despite the perturbed leg being offloaded,

264   indicating the COM experienced a larger downward velocity around toe-off during late stance

265   perturbations (electronic supplementary material, figure S1 and S2). Since the COM during double

266   support is closer to the ground with faster walking speeds [43], this downward velocity may stem from

267   the increased COM velocity caused by the perturbation coinciding with late stance. An additional

268   observation from the perturbed overall leg mechanical energetic responses was differences *among*

269   participants, which was driven primarily by differences in work at the leg/treadmill interface (figure 5C).

270   This emphasizes the need for subject specificity in devices or interventions designed to improve

271   perturbation response.

272   Our third hypothesis was that changes in net ankle work elicited by perturbations would best

273   reflect changes in net overall leg work. Although the energetic demands imposed on the perturbed leg

274   were not as hypothesized, our perturbations nevertheless elicited both generation and dissipation,

275   providing a rich data set to relate leg and joint level mechanical energetics. Our hypothesized

276   contribution by the ankle was supported on the perturbed stride and first recovery stride on the

277   perturbed leg, with a large percentage of the change in work of the perturbed leg being accounted for

278   by the ankle alone (64 and 39% for the perturbed and first recovery stride, respectively). While the

279   importance of the ankle joint in generating mechanical power during steady state walking [21,22,44]

280   and acceleration [26,27,30] has been established, our findings demonstrate that the ankle also plays an

281   important role in mediating transient demands, in agreement with previous studies of human hopping

282   [28]. However, in contrast to the perturbed leg, for the contralateral leg, the knee joint best reflected

283   changes in leg work during the perturbed stride. While previous studies have identified the knee joint as

284   a major contributor during tasks requiring dissipation, such as deceleration and drop landings [27,45],

285   we found that the knee additionally reflected the mechanical work of the leg when generation was

286   required. This could be explained by the knee being a major source of collisional and rebound work in

287   early/midstance, as opposed to the ankle, which primarily contributes later in stance through push-off

288   [37]. Further, previous work that disrupted ankle push-off found that both positive and negative knee

289   energetics were significantly altered [46].

290   One technical limitation of this work was that joint power contributions did not fully account for

291   leg power, particularly during late stance perturbations. These discrepancies may stem from a

292   combination of 1) the use of musculoskeletal model-based inverse dynamics, as opposed to 6 degree of

293   freedom-based inverse dynamics [37–39], and 2) the foot playing a larger role in late stance

294   perturbations [47]. The latter point could be investigated using a musculoskeletal model with free MTP

295   and subtalar joints or using a deformable segment model [40]. Another important limitation of this work

296   was the use of correlations to relate joint and limb level responses. While this approach suggests which

297   joints reflect demands at the leg level, it does not establish whether those joint level responses *cause*

298   changes at the leg level. Future work may further investigate the energetic link between joint and leg

299   level responses by perturbing joint energetics and observing leg level responses, perhaps using wearable

300   robots that inject/extract mechanical energy [48–50]. Further, future studies may also use other flavours

301   of perturbations, such as belt decelerations [13,16,51], external pushes [52], or obstacles [8], to

302   determine whether these findings generalize to other unstable contexts. Lastly, inverse dynamics can

303   only quantify net joint powers and does not capture the contributions of muscle-tendon units to energy

304   exchanges across either side of a joint (*e.g.* coactivation [53]), and between joints (*e.g.* biarticular

305   muscle tendon units [54]) which could be explored using musculoskeletal simulations, electromyography

306   coupled with in-vivo imaging approaches, and animal models [55–57].

307   In conclusion, we have demonstrated that a framework using mechanical energetics can be used

308   to investigate joint level contributions to the energetic demand imposed by a transient treadmill-based

309   perturbation during human walking. We found that the net energetic demand on the perturbed leg

310   during the perturbed stride varied depending on the timing of the perturbation, with changes in net leg

311   work stemming from both changes in power flowing from the leg to the COM and from the leg to the

312   treadmill. The varied energetic demands imposed across timings revealed that the ankle best reflected

313   changes in energetics of the perturbed leg on the perturbed and first recovery strides, while the

314   contralateral knee best reflected changes in energetics of the contralateral leg during the perturbed

315   stride. We anticipate this work will serve as an initial step in understanding the multi-scale contributions

316   to whole body behaviour in unstable contexts.

317

318

319

320   **Ethics.**

321   All participants provided written informed consent and all protocols were approved by the Institutional

322   Review Board at the Georgia Institute of Technology (Protocol H20163).

323   **Data accessibility.**

324   Biomechanical data for all participants (N=7) is available at https://sites.gatech.edu/hpl/archival-data-

325   from-publications/

326   **Authors' contributions.**

327   P.R.G. and G.S.S. conceived of the study and designed the experimental protocol; P.R.G. carried out the

328   experiments, analysed the data, and drafted the manuscript; P.R.G. and G.S.S. edited the manuscript.

329   Both authors gave final approval for publication.

330   **Competing interests.**

331   We declare no competing interests.

332   **Funding.**

335   **Acknowledgements.**

338

References

1. Hartholt KA, Lee R, Burns ER, van Beeck EF. 2019 Mortality From Falls Among US Adults Aged 75 Years or Older, 2000-2016. *JAMA* **321**, 2131. (doi:10.1001/jama.2019.4185)

2. Moreland B, Kakara R, Henry A. 2020 Trends in Nonfatal Falls and Fall-Related Injuries Among Adults Aged ≥65 Years — United States, 2012–2018. *MMWR. Morbidity and Mortality Weekly Report* **69**, 875–881. (doi:10.15585/mmwr.mm6927a5)

3. Burns ER, Stevens JA, Lee R. 2016 The direct costs of fatal and non-fatal falls among older adults — United States. *Journal of Safety Research* **58**, 99–103. (doi:10.1016/j.jsr.2016.05.001)

4. US Bureau of Labor Statistics. 2021 Injuries, Illnesses, and Fatalities Program.

5. Yeoh HT, Lockhart TE, Wu X. 2013 Non-fatal occupational falls on the same level. *Ergonomics* **56**, 153–165. (doi:10.1080/00140139.2012.746739)

6. Berg WP, Alessio HM, Mills EM, Tong C. 1997 Circumstances and consequences of falls in independent community-dwelling older adults. *Age and Ageing* **26**, 261–268. (doi:10.1093/ageing/26.4.261)

7. Talbot LA, Musiol RJ, Witham EK, Metter EJ. 2005 Falls in young, middle-aged and older community dwelling adults: Perceived cause, environmental factors and injury. *BMC Public Health* **5**, 1–9. (doi:10.1186/1471-2458-5-86)

8. King ST, Eveld ME, Martínez A, Zelik KE, Goldfarb M. 2019 A novel system for introducing precisely-controlled, unanticipated gait perturbations for the study of stumble recovery. *Journal of NeuroEngineering and Rehabilitation* **16**, 1–17. (doi:10.1186/s12984-019-0527-7)

9. Grabiner MD, Koh TJ, Lundin TM, Jahnigen DW. 1993 Kinematics of Recovery From a Stumble. *Journal of Gerontology: MEDICAL SCIENCES*. **48**.

10. Debelle H, Harkness-Armstrong C, Hadwin K, Maganaris CN, O'Brien TD. 2020 Recovery From a Forward Falling Slip: Measurement of Dynamic Stability and Strength Requirements Using a Split-Belt Instrumented Treadmill. *Frontiers in Sports and Active Living* **2**, 1–13. (doi:10.3389/fspor.2020.00082)

11. Eng JJ, Winter DA, Patla AE. 1994 Strategies for recovery from a trip in early and late swing during human walking. *Experimental Brain Research* **102**, 339–349. (doi:10.1007/BF00227520)

12. Schillings AM, van Wezel BMH, Mulder T, Duysens J. 2000 Muscular responses and movement strategies during stumbling over obstacles. *Journal of Neurophysiology* **83**, 2093–2102. (doi:10.1152/jn.2000.83.4.2093)

13. Sloot LH, van den Noort JC, van der Krogt MM, Bruijn SM, Harlaar J. 2015 Can treadmill perturbations evoke stretch reflexes in the calf muscles? *PLoS ONE* **10**. (doi:10.1371/journal.pone.0144815)

373 14. Pijnappels M, Bobbert MF, van Dieën JH. 2004 Contribution of the support limb in control of
374   angular momentum after tripping. *Journal of Biomechanics* **37**, 1811–1818.
375   (doi:10.1016/j.jbiomech.2004.02.038)

376 15. Tang PF, Woollacott MH, Chong RKY. 1998 Control of reactive balance adjustments in perturbed
377   human walking: Roles of proximal and distal postural muscle activity. *Experimental Brain
378   Research* **119**, 141–152. (doi:10.1007/s002210050327)

379 16. Roeles S, Rowe PJ, Bruijn SM, Childs CR, Tarfali GD, Steenbrink F, Pijnappels M. 2018 Gait stability
380   in response to platform, belt, and sensory perturbations in young and older adults. *Medical and
381   Biological Engineering and Computing* **56**, 2325–2335. (doi:10.1007/s11517-018-1855-7)

382 17. Li J, Huang HJ. 2021 Small Directional Treadmill Perturbations Induce Differential Gait Stability
383   Adaptation. *Journal of Neurophysiology* (doi:10.1152/jn.00091.2021)

384 18. Donelan JM, Kram R, Kuo AD. 2002 Simultaneous positive and negative external mechanical work
385   in human walking. *Journal of Biomechanics* **35**, 117–124. (doi:10.1016/S0021-9290(01)00169-5)

386 19. Selgrade BP, Thajchayapong M, Lee GE, Toney ME, Chang YH. 2017 Changes in mechanical work
387   during neural adaptation to asymmetric locomotion. *Journal of Experimental Biology* **220**, 2993–
388   3000. (doi:10.1242/jeb.149450)

389 20. Sánchez N, Simha SN, Donelan JM, Finley JM. 2019 Taking advantage of external mechanical work
390   to reduce metabolic cost: the mechanics and energetics of split-belt treadmill walking. *Journal of
391   Physiology* **597**, 4053–4068. (doi:10.1113/JP277725)

392 21. Montgomery JR, Grabowski AM. 2018 The contributions of ankle, knee and hip joint work to
393   individual leg work change during uphill and downhill walking over a range of speeds. *Royal
394   Society Open Science* **5**, 180550. (doi:10.1098/rsos.180550)

395 22. Nuckols RW, Takahashi KZ, Farris DJ, Mizrachi S, Riemer R, Sawicki GS. 2020 Mechanics of walking
396   and running up and downhill: A joint-level perspective to guide design of lower-limb
397   exoskeletons. *PLoS ONE* **15**, 1–20. (doi:10.1371/journal.pone.0231996)

398 23. Alexander N, Strutzenberger G, Ameshofer LM, Schwameder H. 2017 Lower limb joint work and
399   joint work contribution during downhill and uphill walking at different inclinations. *Journal of
400   Biomechanics* **61**, 75–80. (doi:10.1016/j.jbiomech.2017.07.001)

401 24. Lay AN, Hass CJ, Richard Nichols T, Gregor RJ. 2007 The effects of sloped surfaces on locomotion:
402   An electromyographic analysis. *Journal of Biomechanics* **40**, 1276–1285.
403   (doi:10.1016/j.jbiomech.2006.05.023)

404 25. Roberts TJ, Belliveau RA. 2005 Sources of mechanical power for uphill running in humans. *Journal
405   of Experimental Biology* **208**, 1963–1970. (doi:10.1242/jeb.01555)

406 26. Schache AG, Lai AKM, Brown NAT, Crossley KM, Pandy MG. 2019 Lower-limb joint mechanics
407   during maximum acceleration sprinting. *Journal of Experimental Biology* **222**.
408   (doi:10.1242/jeb.209460)

409 27.   Qiao M, Jindrich DL. 2016 Leg joint function during walking acceleration and deceleration. *Journal*
410   *of Biomechanics* **49**, 66–72. (doi:10.1016/j.jbiomech.2015.11.022)

411 28.   Dick TJM, Punith LK, Sawicki GS. 2019 Humans falling in holes: Adaptations in lower-limb joint
412   mechanics in response to a rapid change in substrate height during human hopping. *Journal of*
413   *the Royal Society Interface* **16**. (doi:10.1098/rsif.2019.0292)

414 29.   Daley MA, Felix G, Biewener AA. 2007 Running stability is enhanced by a proximo-distal gradient
415   in joint neuromechanical control. *Journal of Experimental Biology* **210**, 383–394.
416   (doi:10.1242/jeb.02668)

417 30.   Farris DJ, Raiteri BJ. 2017 Modulation of leg joint function to produce emulated acceleration
418   during walking and running in humans. *Royal Society Open Science* **4**. (doi:10.1098/rsos.160901)

419 31.   Zeni JA, Higginson JS. 2010 Gait parameters and stride-to-stride variability during familiarization
420   to walking on a split-belt treadmill. *Clinical Biomechanics* **25**, 383–386.
421   (doi:10.1016/j.clinbiomech.2009.11.002)

422 32.   Liu C, de Macedo L, Finley JM. 2018 Conservation of reactive stabilization strategies in the
423   presence of step length asymmetries during walking. *Frontiers in Human Neuroscience* **12**, 1–13.
424   (doi:10.3389/fnhum.2018.00251)

425 33.   Golyski PR, Vazquez E, Leestma JK, Sawicki GS. 2021 Onset timing of treadmill belt perturbations
426   influences stability during walking. *Journal of Biomechanics* , 110800.
427   (doi:10.1016/j.jbiomech.2021.110800)

428 34.   van den Bogert AJ, Geijtenbeek T, Even-Zohar O, Steenbrink F, Hardin EC. 2013 A real-time
429   system for biomechanical analysis of human movement and muscle function. *Medical and*
430   *Biological Engineering and Computing* **51**, 1069–1077. (doi:10.1007/s11517-013-1076-z)

431 35.   Rajagopal A, Dembia CL, DeMers MS, Delp DD, Hicks JL, Delp SL. 2016 Full-Body Musculoskeletal
432   Model for Muscle-Driven Simulation of Human Gait. *IEEE Transactions on Biomedical Engineering*
433   **63**, 2068–2079. (doi:10.1109/TBME.2016.2586891)

434 36.   Delp SL, Anderson FC, Arnold AS, Loan P, Habib A, John CT, Guendelman E, Thelen DG. 2007
435   OpenSim: Open-source software to create and analyze dynamic simulations of movement. *IEEE*
436   *Transactions on Biomedical Engineering* **54**, 1940–1950. (doi:10.1109/TBME.2007.901024)

437 37.   Zelik KE, Takahashi KZ, Sawicki GS. 2015 Six degree-of-freedom analysis of hip, knee, ankle and
438   foot provides updated understanding of biomechanical work during human walking. *Journal of*
439   *Experimental Biology* **218**, 876–886. (doi:10.1242/jeb.115451)

440 38.   Duncan JA, Kowalk DL, Vaughan CL. 1997 Six degree of freedom joint power in stair climbing. *Gait*
441   *& Posture* **5**, 204–210. (doi:10.1016/S0966-6362(96)01086-7)

442 39.   Buczek FL, Kepple TM, Siegelt KL, Stanhope SJ. 1994 TRANSLATIONAL AND ROTATIONAL JOINT
443   POWER TERMS IN A SIX DEGREE-OF-FREEDOM MODEL OF THE NORMAL ANKLE COMPLEX. *J.*
444   *Biomechanics*. **21**.

445 40.   Takahashi KZ, Kepple TM, Stanhope SJ. 2012 A unified deformable (UD) segment model for
446   quantifying total power of anatomical and prosthetic below-knee structures during stance in gait.
447   *Journal of Biomechanics* **45**, 2662–2667. (doi:10.1016/j.jbiomech.2012.08.017)

448 41.   Cavagna GA, Kaneko M. 1977 Mechanical work and efficiency in level walking and running. *The*
449   *Journal of Physiology* **268**, 467–481. (doi:10.1113/jphysiol.1977.sp011866)

450 42.   Willems PA, Cavagna GA, Heglund NC. 1995 External, internal and total work in human
451   locomotion. *The Journal of experimental biology* **198**, 379–93.

452 43.   Orendurff MS, Segal AD, Klute GK, Berge JS, Rohr ES, Kadel NJ. 2004 The effect of walking speed
453   on center of mass displacement. *Journal of Rehabilitation Research and Development* **41**, 829–
454   834. (doi:10.1682/JRRD.2003.10.0150)

455 44.   Farris DJ, Sawicki GS. 2012 The mechanics and energetics of human walking and running: A joint
456   level perspective. *Journal of the Royal Society Interface* **9**, 110–118. (doi:10.1098/rsif.2011.0182)

457 45.   Yeow CH, Lee PVS, Goh JCH. 2010 Sagittal knee joint kinematics and energetics in response to
458   different landing heights and techniques. *Knee* **17**, 127–131. (doi:10.1016/j.knee.2009.07.015)

459 46.   Huang TWP, Shorter KA, Adamczyk PG, Kuo AD. 2015 Mechanical and energetic consequences of
460   reduced ankle plantar-flexion in human walking. *Journal of Experimental Biology* **218**, 3541–3550.
461   (doi:10.1242/jeb.113910)

462 47.   Takahashi KZ, Worster K, Bruening DA. 2017 Energy neutral : the human foot and ankle
463   subsections combine to produce near zero net mechanical work during walking. *Scientific Reports*
464   , 1–9. (doi:10.1038/s41598-017-15218-7)

465 48.   Witte KA, Fiers P, Sheets-Singer AL, Collins SH. 2020 Improving the energy economy of human
466   running with powered and unpowered ankle exoskeleton assistance. *Sci. Robot.* **5**.

467 49.   Donelan JM, Li Q, Naing V, Hoffer JA, Weber DJ, Kuo AD. 2008 Biomechanical energy harvesting:
468   Generating electricity during walking with minimal user effort. *Science* **319**, 807–810.
469   (doi:10.1126/science.1149860)

470 50.   Shepertycky M, Burton S, Dickson A, Liu Y-F, Li Q. In press. Removing energy with an exoskeleton
471   reduces the metabolic cost of walking.

472 51.   Afschrift M, van Deursen R, de Groote F, Jonkers I. 2019 Increased use of stepping strategy in
473   response to medio-lateral perturbations in the elderly relates to altered reactive tibialis anterior
474   activity. *Gait and Posture* **68**, 575–582. (doi:10.1016/j.gaitpost.2019.01.010)

475 52.   Rong Tan G, Raitor M, Collins SH. 2020 *Bump'em: an Open-Source, Bump-Emulation System for*
476   *Studying Human Balance and Gait*. (doi:10.0/Linux-x86_64)

477 53.   Abbott EM, Nezwek T, Schmitt D, Sawicki GS. 2019 Hurry Up and Get Out of the Way! Exploring
478   the Limits of Muscle-Based Latch Systems for Power Amplification. *Integrative and Comparative*
479   *Biology* **59**, 1546–1558. (doi:10.1093/icb/icz141)

480 54.   Iida F, Rummel J, Seyfarth A. 2008 Bipedal walking and running with spring-like biarticular
481   muscles. *Journal of Biomechanics* **41**, 656–667. (doi:10.1016/j.jbiomech.2007.09.033)

482   55.   Dick TJM, Clemente CJ, Punith LK, Sawicki GS. 2021 Series elasticity facilitates safe plantar flexor
483   muscle-tendon shock absorption during perturbed human hopping. *Proceedings of the Royal*
484   *Society B: Biological Sciences* **288**. (doi:10.1098/rspb.2021.0201)

485   56.   Daley MA, Biewener AA. 2011 Leg muscles that mediate stability: Mechanics and control of two
486   distal extensor muscles during obstacle negotiation in the guinea fowl. *Philosophical Transactions*
487   *of the Royal Society B: Biological Sciences* **366**, 1580–1591. (doi:10.1098/rstb.2010.0338)

488   57.   Lai AKM, Biewener AA, Wakeling JM. 2019 Muscle-specific indices to characterise the functional
489   behaviour of human lower-limb muscles during locomotion. *Journal of biomechanics* **89**, 134–
490   138. (doi:10.1016/j.jbiomech.2019.04.027)
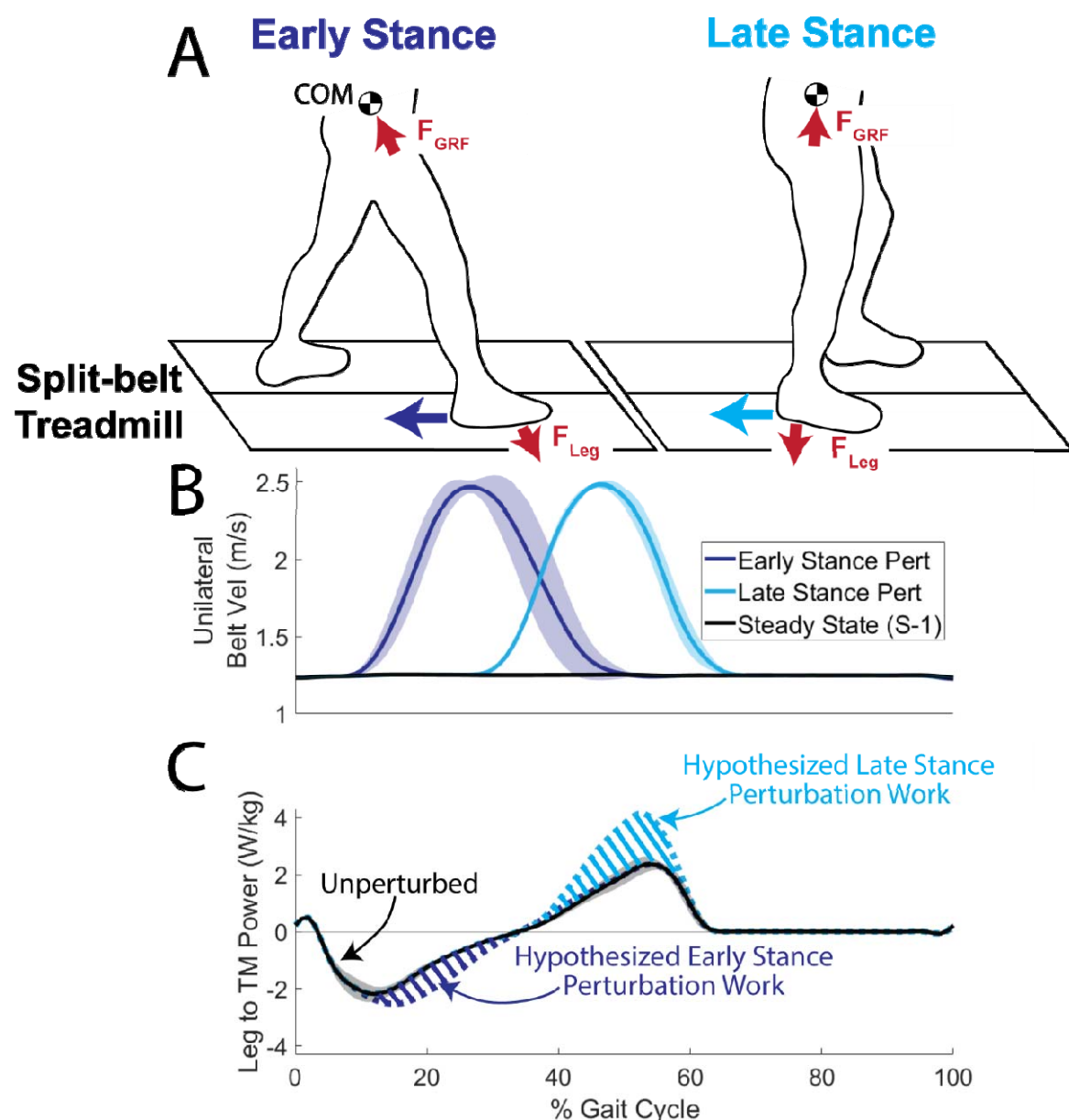
491

492

493

Figure 1 – Perturbation overview. A) Perturbation design. In early stance perturbations, since the leg force is anterior and treadmill velocity is posterior, this results in the leg performing negative work on the belt. In late stance, when leg force is posterior and treadmill velocity is posterior, the leg performs positive work on the belt. B) Unilateral belt velocity traces show across-subject ensemble averages. Shaded regions represent ±1 standard deviation. C) Hypothesized changes in power flowing from the leg to the treadmill relative to steady state, with early stance perturbations eliciting negative power (*e.g.*, dissipation) and late stance perturbations eliciting positive power (*e.g.*, generation).
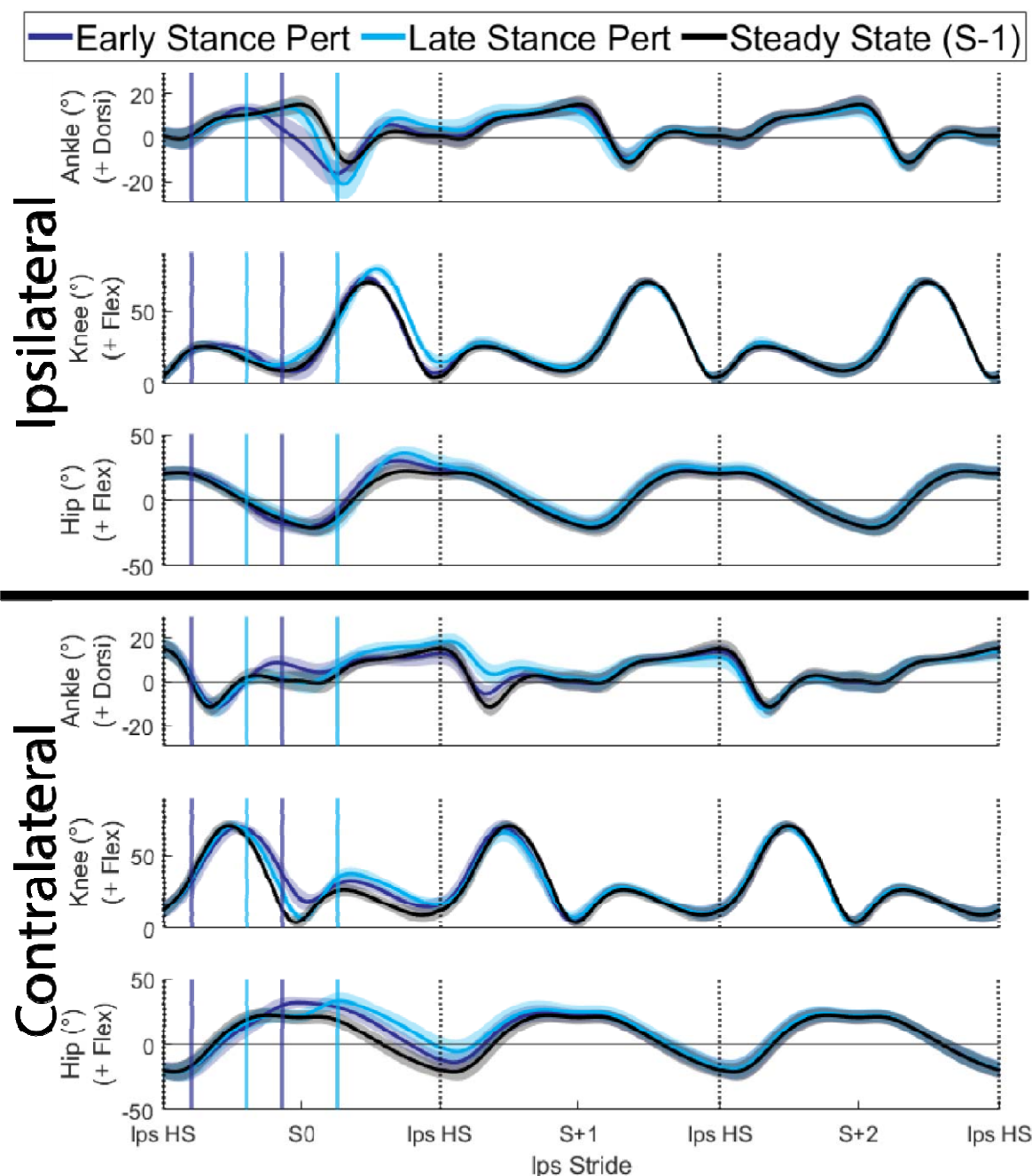
Figure 2 – Lower limb joint angles averaged across subjects and normalized to percentage of the gait cycle. Shaded areas represent ±1 standard deviation. Solid vertical lines indicate the average start and end times of the perturbations. "Steady State" strides are the stride preceding the perturbed stride (S-1).
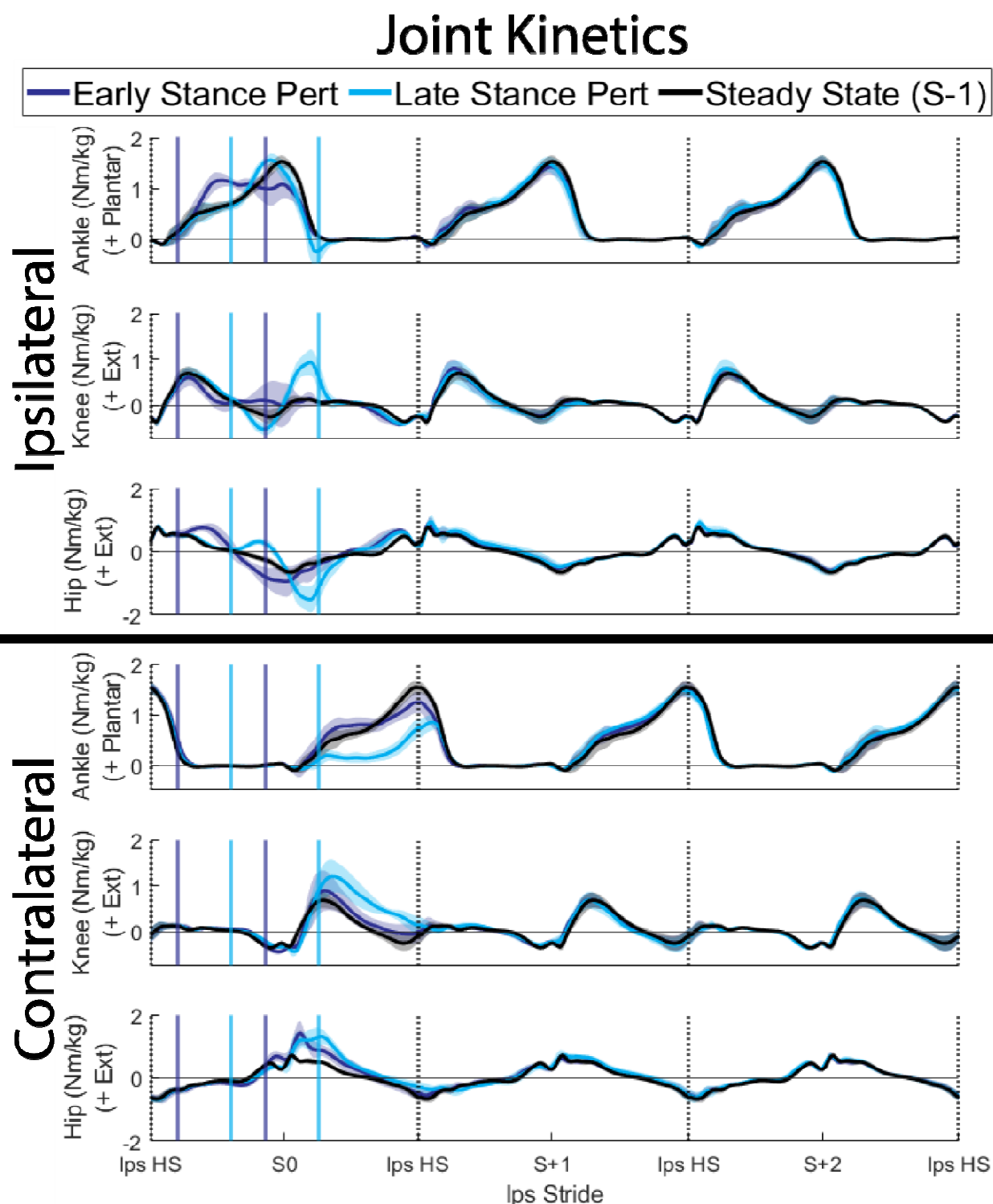
Figure 3 - Lower limb joint moments averaged across subjects and normalized to percentage of the gait cycle. Shaded areas represent ±1 standard deviation. Solid vertical lines indicate the average start and end times of the perturbations. "Steady State" strides are the stride preceding the perturbed stride (S-1).

Figure 4 - Lower limb joint mechanical powers averaged across subjects and normalized to percentage of the gait cycle. Shaded areas represent ±1 standard deviation. Solid vertical lines indicate the average start and end times of the perturbations. "Steady State" strides are the stride preceding the perturbed stride (S-1).
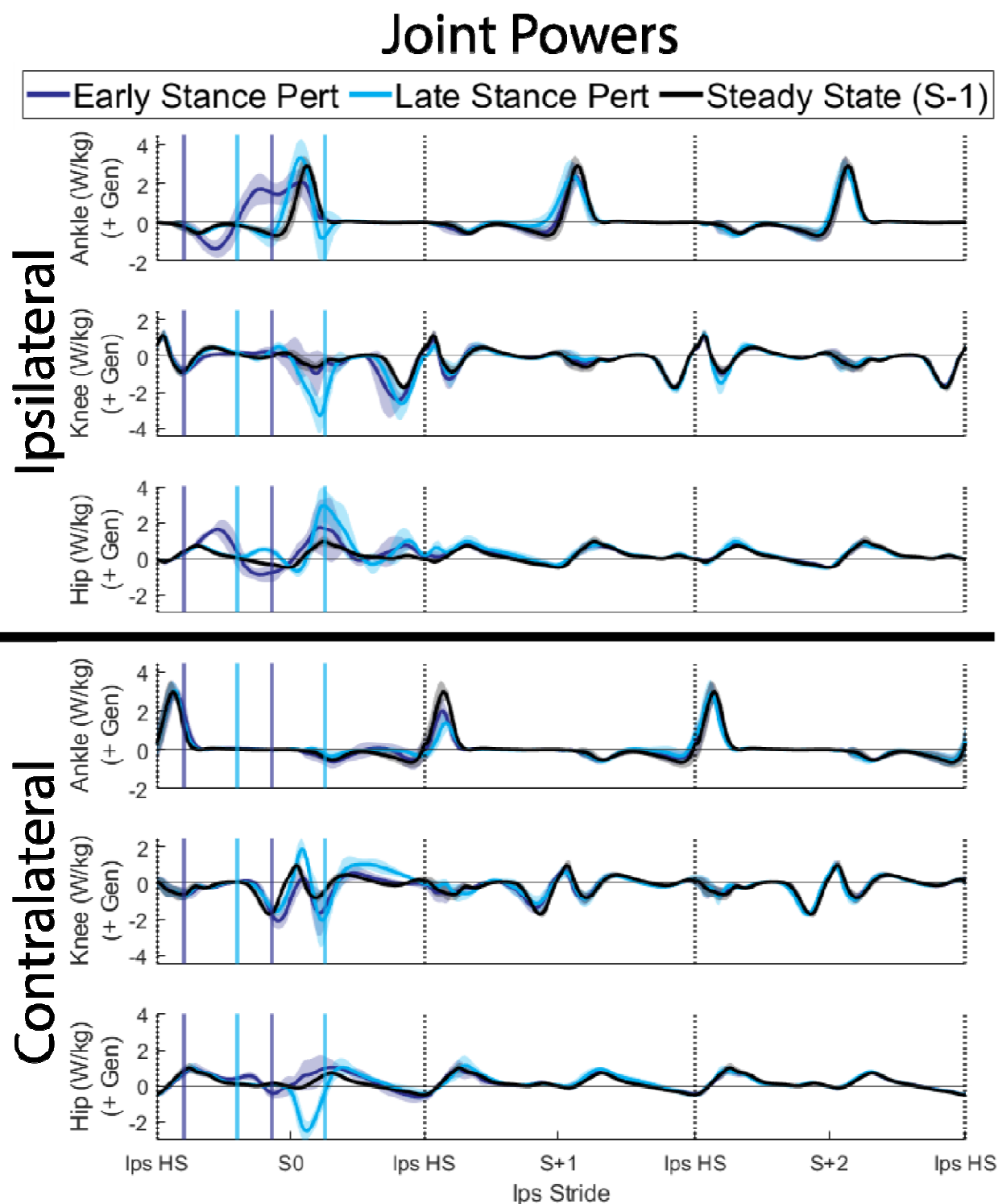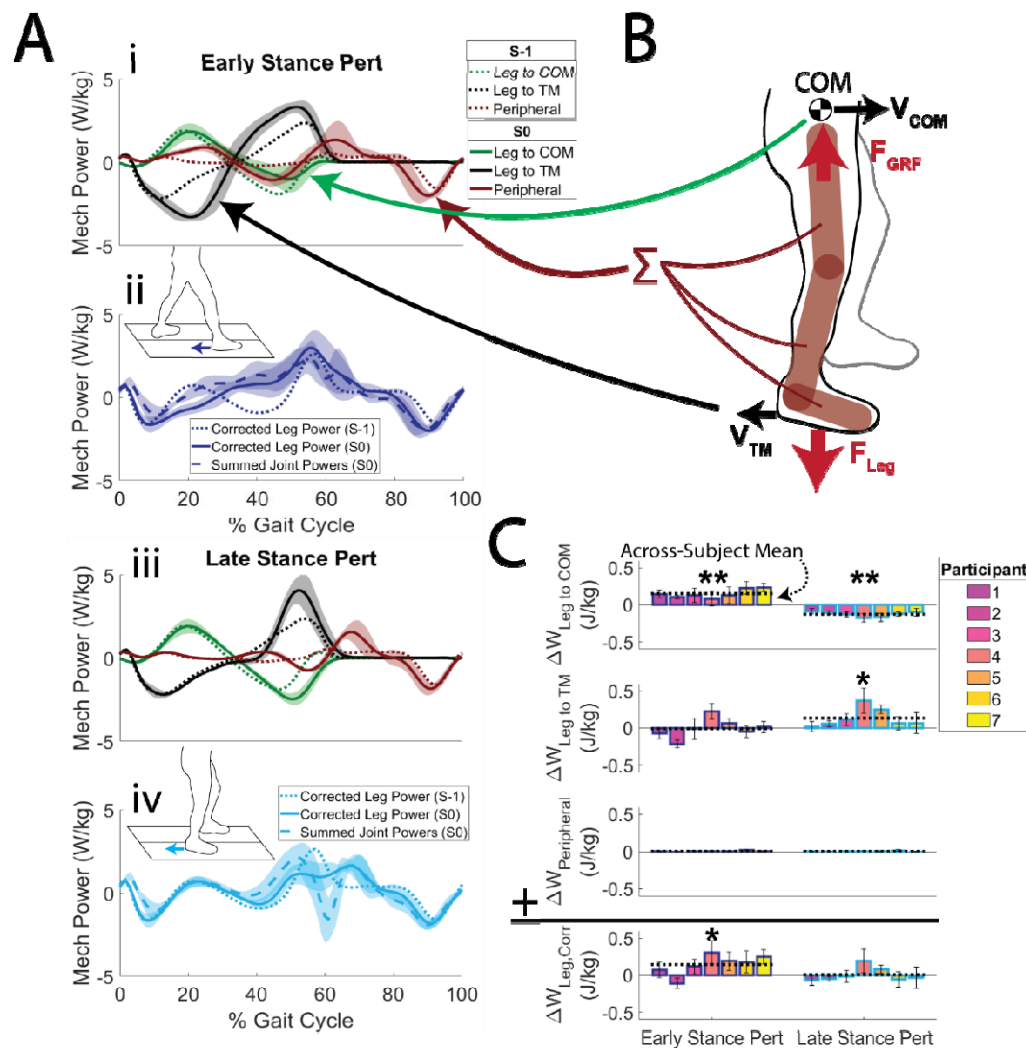
518

Figure 5 – A) Leg mechanical power breakdown for early stance (i and ii) and late stance (iii and iv) perturbations on the ipsilateral leg during the perturbed stride (S0, solid lines), and the unperturbed stride (S-1, dotted lines). For each perturbation timing, across-subject ensemble averages of the contributions to corrected individual leg power are shown (*i.e.*, mechanical power flowing from the leg to the centre of mass, power flowing from the leg to the treadmill, and peripheral power of leg segments moving relative to the centre of mass). These summed contributions (*i.e.*, Corrected Leg Power) are compared with estimated leg power from summing available joint powers (ii and iv). Shaded regions represent ±1 standard deviation. B) Graphical representation of contributions to corrected leg power. As described in section 2.3, power flowing for the leg to the centre of mass or treadmill were the dot product of ground reaction force and centre of mass velocity or leg force and treadmill belt velocity, respectively. Peripheral power contributions were calculated by differentiating the energy of leg segments in time. C) Contributions to corrected leg power were integrated in time to calculate the work contributions over the perturbed stride (S0). These values were subtracted from their respective measurements during steady state strides (S-1) to quantify the changes in mechanical work of these contributions because of the perturbation. Error bars represent ±1 standard deviation. Statistical outcomes represent results of pairwise comparisons of across-subject mean work on the S0 vs. S-1 strides within each timing. * = p < 0.05, ** = p < 0.001
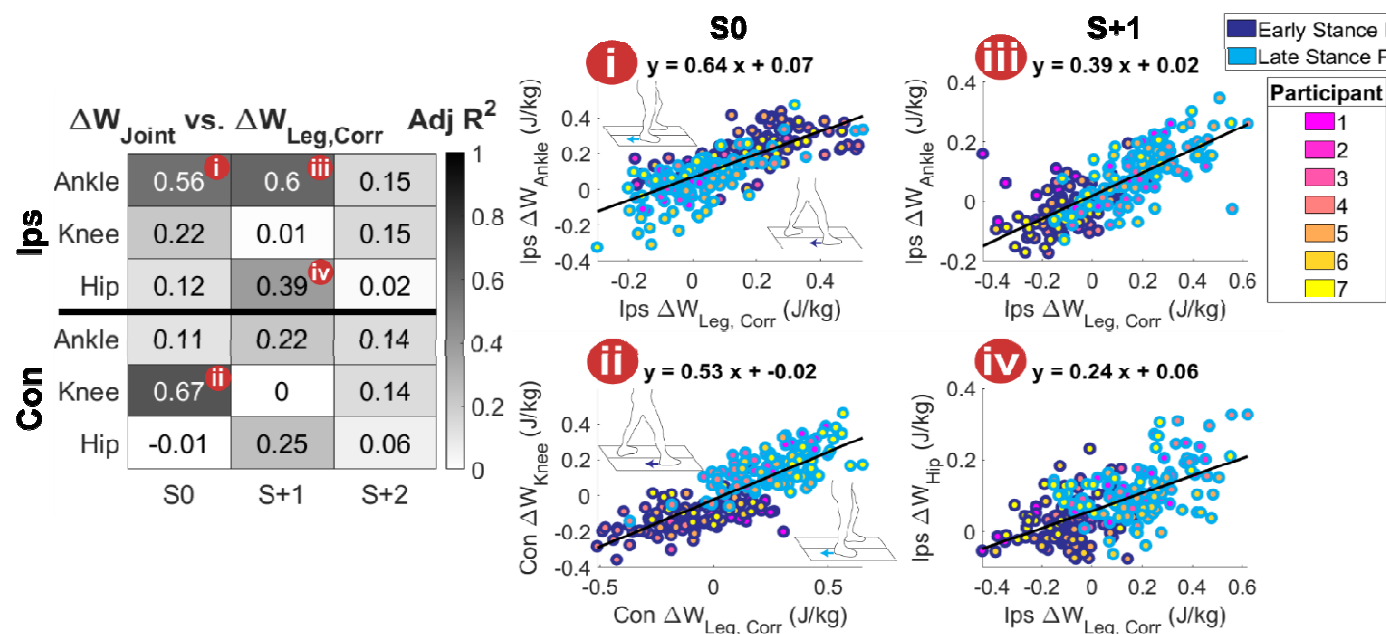
536

Figure 6 – Adjusted R squared values for linear regressions between differences in joint work over a stride from steady state, and differences in corrected leg work over a stride from steady state (S-1) across all 222 perturbations. (i-iv) Scatter plots for joint/stride with the highest adjusted R squared values.

Table S1 – Across-subject mean (standard deviation) peaks in sagittal joint kinematics, kinetics, and mechanical powers. Bold variable names indicate significant

timing x stride interactions. Significant post-hoc tests for the effect of timing are indicated by bold values within stride columns.

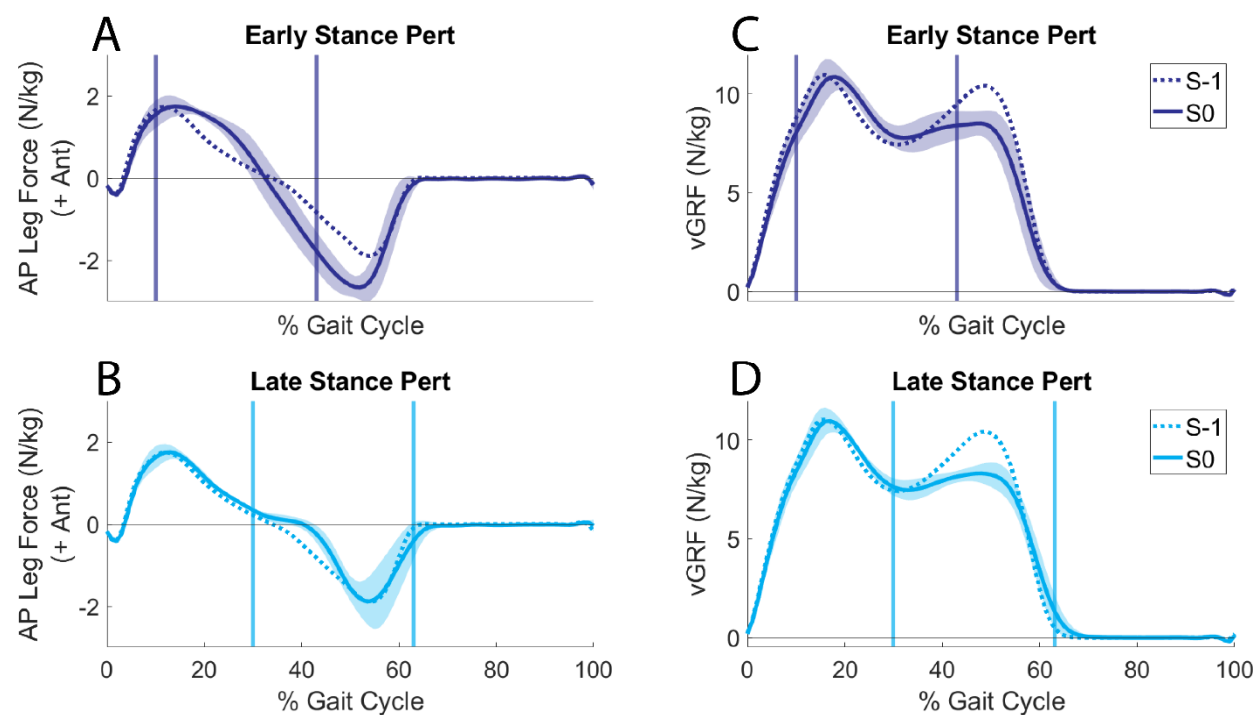|	Ipsilateral Stride:	S-1		S0		S+1		S+2	
	Perturbation Timing:	Early	Late	Early	Late	Early	Late	Early	Late
Ipsilateral	Ankle Dorsiflexion Angle (°)	15.78 (4.16)	15.58 (4.36)	14.53 (2.12)	15.65 (2.49)	15.39 (3.67)	14.59 (3.74)	15.69 (4.32)	14.44 (4.09)
	Ankle Plantarflexion Angle (°)	-11.86 (4.11)	-12.15 (4.6)	-18.26 (4.96)	-23.68 (7.78)	-10.22 (4.5)	-10.89 (4.94)	-11.77 (3.57)	-12.29 (3.95)
	Ankle ROM (°)	27.64 (3.58)	27.73 (3.39)	**32.79 (3.77)**	**39.33 (7.01)**	25.61 (3.33)	25.48 (2.83)	27.46 (4.26)	26.73 (3.11)
	Knee Flexion Angle (°)	70.88 (3.4)	70.93 (3.84)	**74.45 (3.83)**	**81.25 (3.39)**	70.65 (3.5)	69.79 (3.31)	71.1 (3.35)	70.84 (3.68)
	Knee ROM (°)	67.23 (3.33)	67.11 (3.6)	**70.05 (3.25)**	**75.68 (5.55)**	66.56 (3.47)	65.6 (2.7)	67.25 (3.31)	67.12 (3.07)
	Hip Flexion Angle (°)	23.09 (5.73)	22.9 (5.98)	**31 (5.18)**	**37.06 (4.88)**	**25.6 (5.69)**	**28.69 (5.97)**	23.93 (5.57)	25.29 (5.6)
	Hip Extension Angle (°)	-21.48 (6.38)	-21.14 (6.71)	-20.78 (6.9)	-21.64 (6.87)	-19.91 (6.17)	-18.89 (6.64)	-20.59 (6.37)	-20.43 (6.8)
	Hip ROM (°)	44.57 (2.69)	44.04 (2.61)	**51.78 (2.96)**	**58.69 (3.96)**	**45.51 (3.27)**	**47.58 (3.33)**	44.51 (2.5)	45.72 (2.73)
Contralateral	**Ankle Dorsiflexion Angle (°)**	16.19 (4.22)	16.1 (4.37)	**16.89 (3.36)**	**19.37 (3.09)**	**15.57 (3.7)**	**19.29 (3.35)**	15.5 (3.62)	14.67 (4.09)
	Ankle Plantarflexion Angle (°)	-11.56 (3.84)	-12.06 (4.49)	-12 (4.1)	-12.14 (4.7)	**-7.21 (3.48)**	**-1.9 (4.5)**	-12.05 (2.99)	-13.12 (3.99)
	Ankle ROM (°)	27.76 (3.06)	28.17 (3.73)	28.89 (3.44)	31.5 (3.77)	22.79 (2.63)	21.2 (3.66)	27.56 (2.92)	27.78 (3.89)
	Knee Flexion Angle (°)	70.89 (3.79)	70.91 (3.67)	70.67 (3.82)	71.01 (3.5)	**70.17 (4.51)**	**67.4 (6.64)**	70.58 (3.9)	70.48 (3.66)
	Knee ROM (°)	67.07 (3.69)	67.04 (3.42)	**60.82 (4.11)**	**66.08 (3.22)**	**65.62 (3.83)**	**61.91 (6.76)**	66.65 (3.68)	66.74 (3.69)
	Hip Flexion Angle (°)	22.76 (5.78)	22.85 (5.93)	33.78 (3.71)	34.24 (6.24)	24.85 (6.29)	27.64 (6.76)	23.6 (5.79)	24.33 (5.73)
	Hip Extension Angle (°)	-21.21 (6.87)	-21.52 (6.48)	-21.13 (7.07)	-21.61 (6.53)	-18.71 (6.96)	-17.94 (6.71)	-20.4 (7.12)	-20.23 (6.73)
	Hip ROM (°)	43.97 (2.79)	44.37 (2.56)	54.9 (4.16)	55.85 (3.55)	43.56 (2.81)	45.58 (2.72)	44 (3.24)	44.55 (2.58)
Ipsilateral	**Ankle Plantarflexion Moment (Nm/kg)**	1.55 (0.12)	1.56 (0.13)	**1.48 (0.14)**	**1.7 (0.08)**	1.5 (0.13)	1.57 (0.13)	1.54 (0.12)	1.54 (0.14)
	Knee Extension Moment (Nm/kg)	0.71 (0.15)	0.72 (0.18)	**0.69 (0.16)**	**1.23 (0.3)**	0.85 (0.17)	0.77 (0.24)	0.73 (0.14)	0.84 (0.18)
	Knee Flexion Torque (Nm/kg)	-0.45 (0.08)	-0.46 (0.09)	-0.54 (0.11)	-0.64 (0.1)	-0.47 (0.07)	-0.49 (0.09)	-0.46 (0.07)	-0.45 (0.07)
	Hip Extension Moment (Nm/kg)	0.82 (0.1)	0.82 (0.1)	0.94 (0.11)	0.88 (0.12)	1.06 (0.15)	1.1 (0.2)	**0.85 (0.1)**	**1.01 (0.12)**
	Hip Flexion Torque (Nm/kg)	-0.7 (0.09)	-0.69 (0.11)	**-1.18 (0.45)**	**-1.85 (0.45)**	-0.59 (0.08)	-0.58 (0.1)	-0.65 (0.1)	-0.68 (0.11)
Contralateral	Ankle Plantarflexion Moment (Nm/kg)	1.58 (0.13)	1.58 (0.12)	1.56 (0.11)	1.53 (0.11)	1.54 (0.14)	1.52 (0.1)	1.57 (0.14)	1.55 (0.13)
	Knee Extension Moment (Nm/kg)	0.72 (0.16)	0.71 (0.18)	**1.06 (0.34)**	**1.35 (0.37)**	0.76 (0.12)	0.75 (0.16)	0.73 (0.16)	0.75 (0.15)
	Knee Flexion Torque (Nm/kg)	-0.45 (0.08)	-0.45 (0.08)	-0.55 (0.07)	-0.64 (0.15)	-0.44 (0.07)	-0.44 (0.08)	-0.45 (0.08)	-0.45 (0.07)
	Hip Extension Moment (Nm/kg)	0.82 (0.09)	0.81 (0.1)	1.85 (0.34)	1.81 (0.15)	0.83 (0.11)	0.97 (0.12)	0.82 (0.11)	0.83 (0.09)
	Hip Flexion Torque (Nm/kg)	-0.7 (0.11)	-0.71 (0.1)	-0.71 (0.13)	-0.71 (0.1)	-0.67 (0.12)	-0.64 (0.14)	-0.66 (0.11)	-0.67 (0.14)
Ipsilateral	**Ankle Generation Power (Watts/kg)**	3.29 (0.49)	3.33 (0.49)	**3.22 (0.83)**	**4.37 (0.94)**	2.97 (0.5)	3.13 (0.52)	3.18 (0.54)	3.14 (0.45)
	Ankle Dissipation Power (Watts/kg)	-0.91 (0.25)	-0.89 (0.17)	**-1.65 (0.41)**	**-2.63 (1.57)**	-0.99 (0.19)	-0.72 (0.15)	-0.95 (0.27)	-0.98 (0.19)
	Knee Generation Power (Watts/kg)	1.26 (0.28)	1.27 (0.23)	1.4 (0.18)	1.31 (0.22)	**1.23 (0.4)**	**1.03 (0.33)**	1.23 (0.3)	1.35 (0.31)
	Knee Dissipation Power (Watts/kg)	-1.87 (0.11)	-1.89 (0.14)	**-3.34 (1.41)**	**-4.86 (1.35)**	-2 (0.19)	-2.05 (0.3)	-1.8 (0.12)	-2.11 (0.29)
	Hip Generation Power (Watts/kg)	1.15 (0.27)	1.12 (0.26)	**2.8 (1.66)**	**4.07 (1.42)**	1.17 (0.31)	1.41 (0.26)	1.1 (0.27)	1.16 (0.28)
	Hip Dissipation Power (Watts/kg)	-0.59 (0.09)	-0.55 (0.1)	-1.36 (0.29)	-1.23 (0.59)	-0.54 (0.12)	-0.5 (0.1)	-0.54 (0.09)	-0.62 (0.13)
Contralateral	Ankle Generation Power (Watts/kg)	3.34 (0.64)	3.3 (0.53)	3.35 (0.5)	3.31 (0.5)	2.44 (0.76)	1.92 (0.42)	3.16 (0.54)	3.15 (0.63)
	Ankle Dissipation Power (Watts/kg)	-0.92 (0.22)	-0.9 (0.19)	**-1.2 (0.26)**	**-0.78 (0.18)**	-0.91 (0.26)	-0.86 (0.13)	-0.84 (0.15)	-0.88 (0.16)
	Knee Generation Power (Watts/kg)	1.26 (0.25)	1.22 (0.21)	**1.17 (0.42)**	**3.31 (0.56)**	1.18 (0.18)	1.2 (0.22)	1.26 (0.24)	1.25 (0.23)
	Knee Dissipation Power (Watts/kg)	-1.85 (0.1)	-1.84 (0.13)	-3.04 (0.77)	-3.38 (1.55)	-1.84 (0.16)	-1.72 (0.18)	-1.81 (0.09)	-1.91 (0.09)
	Hip Generation Power (Watts/kg)	1.14 (0.26)	1.13 (0.26)	1.81 (0.71)	1.61 (0.43)	1.22 (0.37)	1.44 (0.46)	1.07 (0.23)	1.11 (0.25)
	Hip Dissipation Power (Watts/kg)	-0.58 (0.08)	-0.58 (0.09)	**-1.1 (0.32)**	**-3.66 (0.48)**	-0.67 (0.2)	-0.65 (0.22)	-0.57 (0.12)	-0.6 (0.14)

Figure S1 – (A-B) Anteroposterior forces exerted by the ipsilateral leg, and (C-D) vertical ground reaction forces of the ipsilateral leg exerted on the COM on the perturbed stride (S0) and preceding unperturbed stride (S-1). Solid vertical lines indicate the average start and end times of the perturbations.
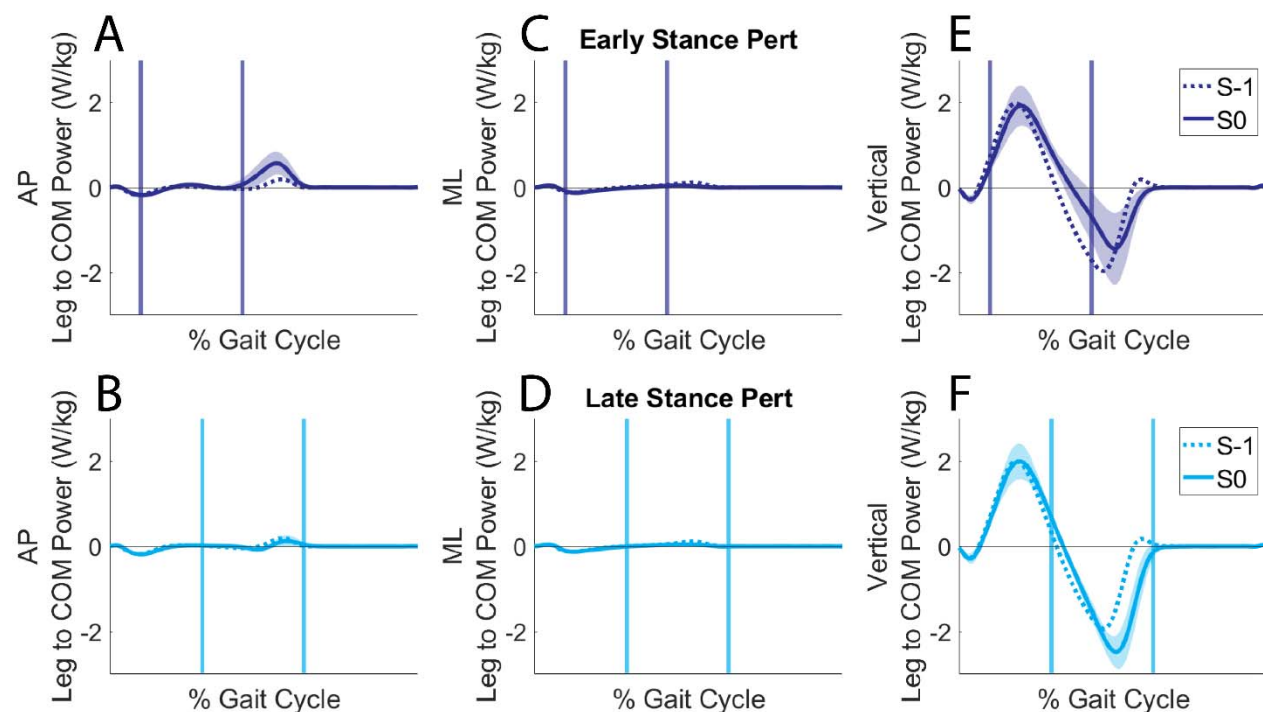
Figure S2 – Mechanical power flowing from the perturbed leg to the COM separated into (A-B) anteroposterior, (C-D), mediolateral, and (E-F) vertical contributions during the perturbed stride (S0) and preceding unperturbed stride (S-1). Solid vertical lines indicate the average start and end times of the perturbations.